Imaging in pre-clinical cancer research : applied to bone metastases
Snoeks, T.J.A.

Cover Page

The handle http://hdl.handle.net/1887/19081 holds various files of this Leiden University dissertation.

Author: Snoeks, Thomas Jan Adriaan
Title: Imaging in pre-clinical cancer research : applied to bone metastases
Date: 2012-06-13

2

Normalized Volume of Interest Selection and Measurement of Bone Volume in μCT Scans

Thomas J.A. Snoeks [1]
Eric L. Kaijzel [1]
Ivo Que [1]
Isabel M. Mol [1]
Clemens W.G.M. Löwik [1]
Jouke Dijkstra [2]

[1]Dept. of Endocrinology, LUMC, Leiden, The Netherlands
[2]Dept. of Radiology, Division of Image Processing LKEB, LUMC, Leiden, The Netherlands

Abstract

Quantification of osteolytic lesions in bone is pivotal in the research of metastatic bone disease in small animal models. Osteolytic lesions are quantified using two dimensional X-ray photographs, which often neglects to take into account any changes in three dimensional structure. Furthermore, measurement errors are inadvertently introduced when a region of interest with predefined dimensions is used during µCT analysis. To study osteolytic processes, a normalized method of selecting a region of interest is required. Here we describe a new method to select volumes of interest in a normalized way regardless of curvature, fractures or dislocations within the bone. In addition, this method enables the user to visualize normalized cross-sections in an exact 90° angle or along the longitudinal axis of bone, at any given point. As a result, the user can compare measurements of diameter, volume and structure between different bones in a normalized manner.

Introduction

Certain types of cancer preferentially metastasize to bone. In cases of breast cancer, *post mortem* examination revealed that over 70% of the patients carried bone metastases.[1] Bone metastases are the cause of severe morbidity.[2–4] As a result, much research is being conducted toward an optimal treatment regimen. Therefore, quantification of osteolytic lesion size and treatment evaluation in small animal models are pivotal for preclinical research in being able to characterize metastatic bone disease.

At present, osteolytic lesions are quantified using two dimensional (2D) radiographs.[5,6] The scoring of radiographs is performed by manual drawing of a region of interest (ROI) around the lesion, a method prone to observer bias. This procedure cannot be automated because of high variability of shape and grey-values of the bones and lesions. The grey-value intensity of the lesion depends heavily on the location of the lesion and the chance of multiple lesions being projected on top of each other. The shape of the bone itself can be altered drastically due to fractures or the bone can even be partially destroyed in case of severe osteolytic lesions, making the reproducible selection of a ROI more difficult. Small lesions and subtle changes in bone thickness are not visible or easily overlooked.

µCT scans provide three dimensional (3D) structural information which allows a more exact assessment of the disease-induced changes. In contrast to conventional radiography, µCT scans can be used to quantify both the decrease in bone volume in case of osteolysis as well as the increase in bone volume in case of osteoblastic lesions. However, analysis of µCT scans is difficult and time consuming.

A normalized method of selecting a region of interest is required in order to study volumetric changes. The murine tibia for instance, is slightly curved in a healthy state. This curved shape makes it impossible to make a µCT scan composed entirely of slices that are perpendicular to the center-line of the bone. In the case of severe osteolysis, parts of the bone might be missing or fractured increasing the complexity of volume of interest (VOI) selection. Therefore, the µCT scan must be reformatted in order to be able to perform a normalized selection of a VOI independent of the scan orientation.

Here we describe a new method to reformat µCT scans and select a VOI in a normalized way regardless of curvature, fractures or dislocations within the bone. This method makes use of curved planar reformation along a center-line defined by the user. The selection of the VOI was performed in this reformatted µCT scan. To prevent any measurement errors introduced by the reformation, the actual volume measurements of the selected VOI are performed in the original scan volume. In addition, we can visualize normalized cross-sections at an exact 90° angle or along the longitudinal axis of bone, at any given point. This method allows side-by-side visualizations of cross-sections and enables the comparison of diameter and volume measurements between different scans in a normalized manner.

Materials & methods

Animals

Female athymic mice (BALB/c nu/nu, 5 weeks old) mice were acquired from Charles River (Charles River, L'Arbresle, France), housed in individually ventilated cages while food and water were provided *ad libitum*. All surgical and analytical procedures were performed under isoflurane gas anesthesia. At the end of the experimental period, animals were sacrificed by cervical dislocation. Animal experiments were approved by the local committee for animal health, ethics and research of Leiden University Medical Center.

Cell lines & culture conditions

The MDA-231-B/Luc+ cell line (hereafter MDA-BO2), a bone-seeking and luciferase-expressing subclone from the human breast cancer MDA-MB-231,[7,8] was cultured in DMEM (Invitrogen, Carlsbad, CA USA) containing 4.5 g glucose/l supplemented with 10% fetal calf serum (FCS) (Lonza, Basel, Switzerland), 100 units/ml penicillin, 50 μg/ml streptomycin (Invitrogen) and 800 μg/ml geneticin/G418 (Invitrogen). Cultures were maintained in a humidified incubator at 37°C and 5% CO_2.

Experimental setup

Intra-osseous inoculations with MDA-BO2 cells and sham operations; Mice received an intra-osseous inoculation with MDA-BO2 cells ($n = 8$) into the right tibia as described previously.[8] After 42 days, mice were sacrificed by cervical dislocation and the hind limbs were fixed overnight in 4% formaldehyde. Mice in the sham operated group (partial bone marrow ablation) underwent the same procedure as the MDA-BO2 inoculated animals except that the intra-osseous injection contained only PBS and no tumor cells. After 10 and 42 days mice were sacrificed by cervical dislocation ($n = 5$), the hind limbs were fixed.

Bisphosphonate treatment

Mice received daily sub-cutaneous injections with risedronic acid (150 μg/kg/day) or a similar volume of PBS ($n = 6$). After 42 days mice were sacrificed by cervical dislocation, the left hind limbs were fixed.

Radiograph and μCT analysis

After the experimental period, the hind limbs of all mice with a tumor were analyzed by radiography (Kodak X-OMAT TL film, Eastman Kodak Company, Rochester, NY USA) using a Faxitron 43805 X-ray system (Hewlett-Packard, Sunnyvale, CA USA).

The radiographs were digitized and subsequently analyzed using Adobe Photoshop CS3 V10.0.1 (Adobe Systems, San Jose, CA USA).

After the experimental period, µCT scans of the fixed hind limbs were made using a SkyScan 1076 µCT scanner (SkyScan, Kontich, Belgium) using a source voltage and current set to 40 kV and 250 µA, with a step size of 0.9° over a trajectory of 180°. Images were taken with an image pixel size of 9.03 µm and a frame averaging of 3 to reduce noise. Reconstructions were made using nRecon V1.6.2.0 software (SkyScan) with a beam hardening correction set to 20% and a ring artifact correction set to 5. Processing, volume measurements and visualizations were performed using MeVisLab V1.6 (MeVis Medical Solutions AG, Bremen, Germany). All µCT scans presented here were made using an identical scanning protocol and reconstructed with identical settings.

The method is very similar to the analysis of coronary arteries in CT angiography images using multi-plane reformatting. First, a center-line through the bone was defined. To do this, the user indicated manually the location of the center-line on several slices throughout the original 3D data set (hereafter referred to as the original space) after which a cubic B-spline was fitted through these points. Next, regular spaced planes perpendicular to the center-line were extracted. These planes were stacked into a new volume (hereafter referred to as the reformatted space). The user defined a VOI by indicating a start and an end plane relative to anatomical features in the reformatted space. These cut-off planes were transformed back into the original space after which a region grower, initiated at a single or multiple seed point(s) was used to select bone material. All connected voxels above a certain threshold value were considered as bone. For the scans presented here, a lower threshold of 50 and an upper threshold of 255 were used. Multiple seed points were needed in case there was fractured bone. This threshold value was determined using the best separation value from the intensity histogram and kept constant for all of the scans used within these experiments. The region grower was set to stop when no further connected voxels met the bone criterion or at the cut-off planes indicated by the user. This method can be used for µCT datasets acquired using a different scanning protocol, scanner or reconstruction parameters. In which case, threshold values would be required to be optimized.

Results

All the reconstructed scans underwent a first visual assessment to check the quality of the data sets. None of the scans contained obvious scanning artifacts which would interfere with later analysis.

Center-line definition and generation of normalized cross-sections

The definition of a center-line is the pivotal first step of the analysis method. All further steps and volume measurements are performed relative to this center-line. The

center-line is calculated using several center points throughout the scan, indicated manually by the user.

A center-line was successfully fitted through each of the scans. This center-line was used to render cross-sections and longitudinal sections from the original space. The orientation of the section planes was relative to the center-line, even though the actual sections were generated from the original scan data (Figure 2.1). These normalized cross-sections and longitudinal sections can be generated anywhere along the center-line. Such normalized visualizations allow for side-by-side comparison between multiple scans or between scans and histological sections.

Using a reformatted space to define a normalized volume of interest

A reformatted space is used to define a VOI relative to the bone architecture in multiple scans, regardless of scan orientation or changes to the original bone anatomy. The reformatted space was generated by straightening the center-line and reformatting the rest of the scan around the new center-line accordingly. After selecting a normalized VOI in this reformatted space, the VOI was mapped back to the original scan space. This allowed the user to conduct measurements without distortion of the data due to the reformatting steps.

To generate the reformatted space, regular spaced planes perpendicular to the center-line were extracted from the original scan volume and stacked to form a new, normalized, volume. In this new volume, the naturally curved bone was straightened and orientated along the z-axis of the new stack regardless of its shape and position in the original volume. Longitudinal sections of this reformatted bone could be rendered and used for the assessment of the cortical thickness along the whole bone (Figure 2.2a–c). In contrast to visualizations based on the original scan data, the visualizations based on the reformatted data did not have artifacts resulting from the angle between the bone and the sectioning plane.

The new reformatted space allowed the user to navigate through the scans and locate positions relative to dominant anatomical features. For volume measurements, the VOI was defined by two cut-off planes perpendicular to the bone. Throughout these studies, the knee and the branch point between the tibia and fibula were used as dominant anatomical features relative to which these cut-off planes were defined. The cut-off planes were transformed back into the original space where the actual volume was determined using a region grower with a threshold set for calcified tissue (Figure 2.2d–e).

The center-line definition and generation of a reformatted space was tested on a scan of a more complex pathological case. This was also to evaluate the performance of the method in more extreme conditions. A scan of a fractured dislocated bone with a callus was used to generate a complex dataset. A reformatted space was generated and used to produce longitudinal cross-sections regardless of the fracture, dislocation and callus (Figure 2.3).
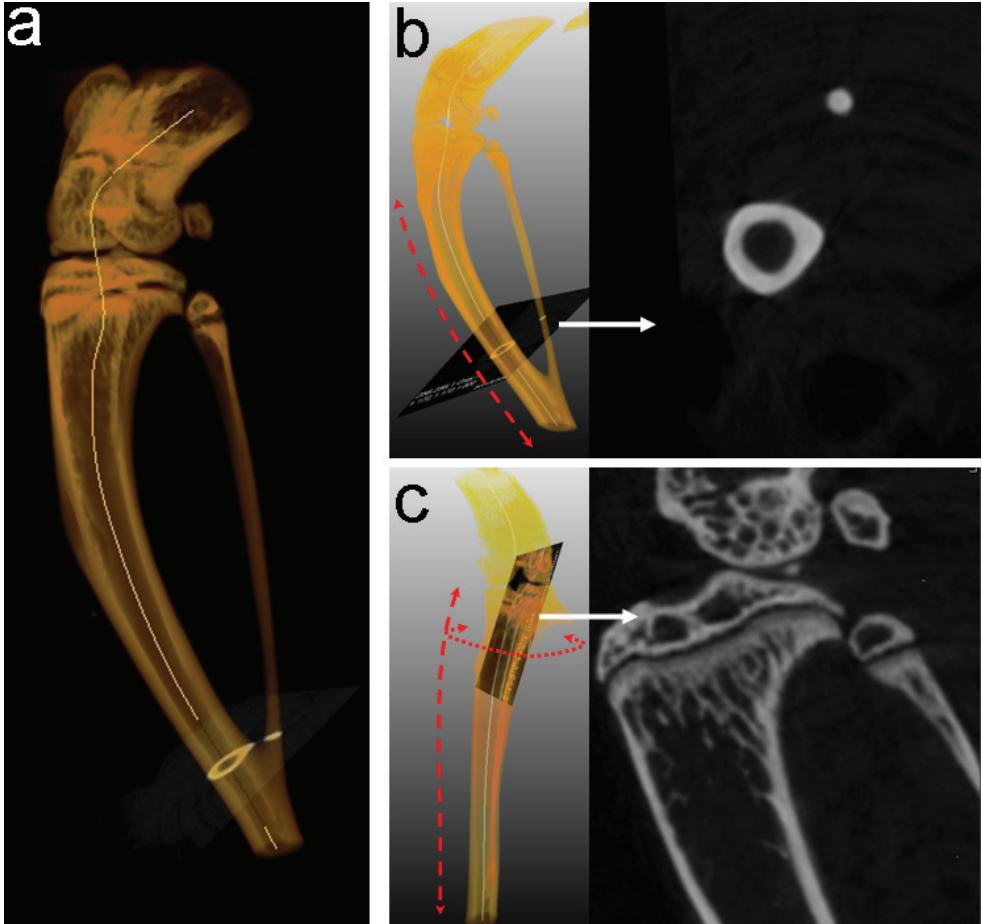
Figure 2.1: Fitting a spline and rendering cross-sections. (a) Semi transparent reconstruction of the original scan volume with a global threshold set for bone. Several center points were indicated manually and a spline has been fitted through these points. (b) Transversal cross-sections can be generated perpendicular to the center-line at any point along the center-line. Since the center-line follows the curvature of the bone, these cross-sections will always be perpendicular, i.e. in a 90° angle, to the bone. These cross-sections can be used for exact side-by-side comparison of the same section between different scans. (c) In a similar fashion, osculating planes can be generated anywhere along the center-line resulting in longitudinal cross-sections of the original scan volume. The spline tangent vector at the point of intersection with the longitudinal sectioning plane then forms the axis of rotation of the plane.
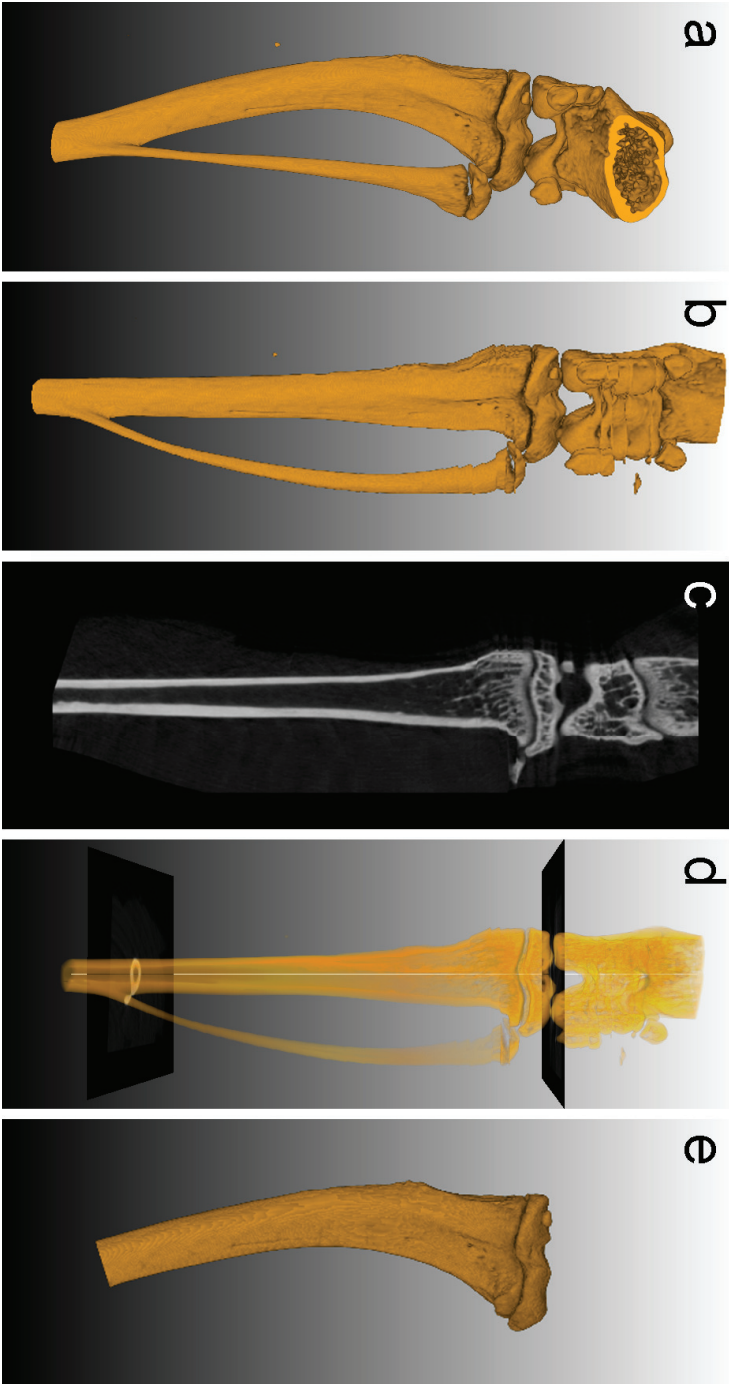
Figure 2.2: Selecting a VOI using orthogonal cross-sections. (a) 3D rendering of the original scan volume. (b) 3D rendering of the complete image stack of perpendicular cross-sections generated along the center-line (generated as shown in Figure 2.1). (c) Longitudinal cross-section generated from the reformatted space. The sectioning plane can be rotated along the longitudinal axis. These sections can be used for side-by-side comparison between different scans. (d) Definition of transversal cut-off planes using the reformatted space to calculate the relative position between the knee and the branch point of the fibula and tibia. (e) 3D rendering of a VOI. The volume was selected in the original space using a region grower limited by the cut-off planes which were mapped back from the reformatted space.
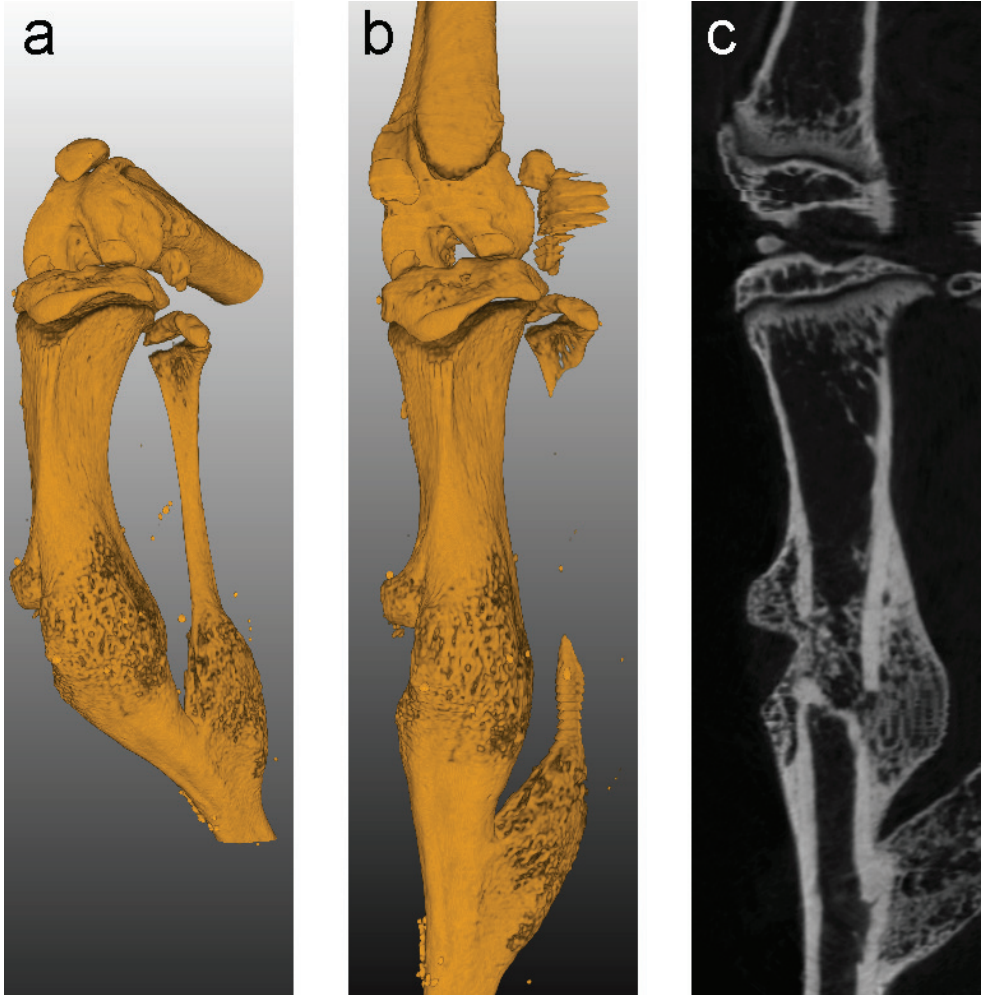
Figure 2.3: Generation of a reformatted space in a more severe pathological case. (a) Original scan volume. (b) Volume rendering of the reformatted space. (c) Longitudinal cross-section generated from the reformatted space. The reformatted space contains some artifacts due to the planar reformation. These artifacts have no influence on the measured bone volume since all actual measurements are performed within the original scan data.

Volume measurements using normalized volumes of interest

Next, the variability between observations was assessed to demonstrate that the VOI selection and volume measurement could be reproduced. In addition, we showed that the volume measurements could be used to quantify biologically relevant changes in bone volume.

To test the precision of the selection and quantification of a VOI, the center-line definition and volume measurements of mouse tibiae were repeated ten times on the same bone on ten different days performed by the same observer. The measured bone volume was the tibial volume between the knee and the branch point of the tibia and fibula, but not including the fibula (as shown in Figure 2.2e). The coefficient of variation (cv) of these ten repeated measurements, defined as the ratio of the standard deviation to the mean, was 0.001 indicating the low variation between observations.

To evaluate whether these volume measurements could be used to identify differences in bone volume, the tibial bone volumes of the left tibiae of risedronic acid treated mice were compared to that of untreated control mice of identical background, sex and age. The tibia was selected by placing two cut-off planes in the reformatted space, one through the knee and a second one at the branch point between the tibia and fibula. The fibula was not included in the VOI. Bone volume increased by approximately 22% (from $7.82mm^3 \pm 0.22$ to $9.58mm^3 \pm 0.58$) after treatment with risedronic acid. The longitudinal cross-sections indicate the increase in trabecular bone volume (Figure 2.4a).

Influence of intra-osseous inoculation on volume measurements

Intra-osseous inoculation of tumor cells is a method commonly used to study bone metastasis of cancer.[9] During the intra-osseous procedure the bone marrow is partially flushed out of the bone. This partial bone marrow ablation has profound effects on the local bone turnover. One week after ablation, the bone formation induced from ablation of bone marrow reaches a maximum. After the first week, the bone volumes had normalized over time as the bone recovered from the procedure.[10,11] We evaluated the effects of intra-osseous inoculation procedure on volume measurements of various VOIs to see how much it would interfere with the measurement of tumor-induced volumetric changes.

Four different VOI definitions were used to gain an insight in the location of volumetric changes; (1) the tibia from the branch point with the fibula up to the knee (referred to as whole bone), (2) the distal half of the whole bone volume (referred to as lower half), (3) the proximal half of the whole bone volume (referred to as upper half) and (4) the proximal 25% of the whole bone volume (referred to as the upper quarter).

The measurements were performed on a group of ten mice which received a sham operation with PBS on the right tibiae following the protocol of intra-osseous injection of cancer cells. The left tibiae were used as untreated controls. The mice were sacrificed at 10 and 42 days after the procedure. The volume increase was defined
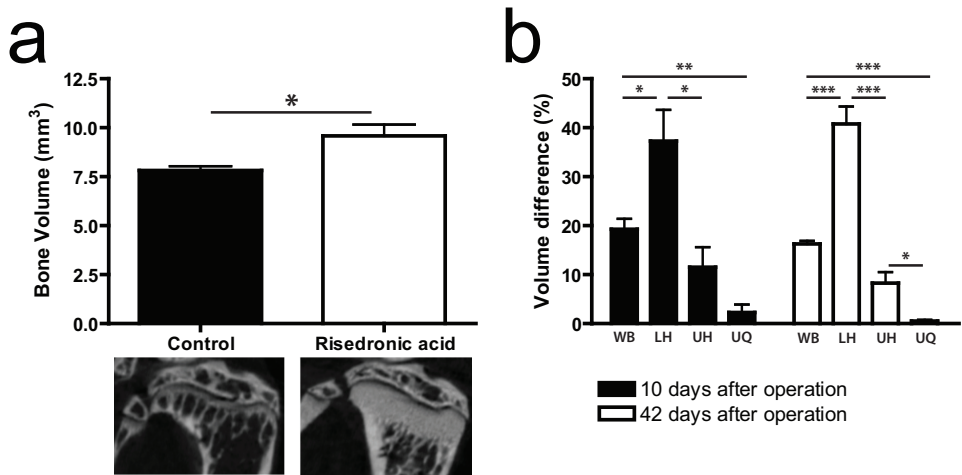
Figure 2.4: Quantification of various volumes of interest. (a) Tibial volumes of saline treated controls and risedronic acid treated animals after 42 days of treatment. The volumes of the tibiae increased with approximately 22%, from $7.82\text{mm}^3 \pm 0.22$ to $9.58\text{mm}^3 \pm 0.58$. The increase in trabecular bone volume can be appreciated form the detailed cross-sections of the epiphysis. Error bars indicate SEM, $* : p < 0.05$. (b) The effect of bone marrow ablation on healthy animals. The graph shows the relative difference in bone volume between bones after a partial bone marrow ablation (right hind limbs) compared to untreated control bones (left hind limbs) 10 days and 42 days after the surgical procedure. The whole bone (WB), lower half (LH) upper half (UH) and upper quarter (UQ) were measured in the same set of scans for comparison. The effect of bone marrow ablation was less toward the proximal end of the bone bath after 10 and 42 days. Error bars indicate SEM, $* : p < 0.05, ** : p < 0.01, *** : p < 0.001$.

as a difference in percentage compared to the whole bone volume. The whole bone volume increased approximately 19.5% (± 2.1) within the first ten days after bone marrow ablation. This relative volume increase was not the same for every region of the bone. In the lower half, the volume increase was approximately 37.2% (± 6.2) after 10 days, this was approximately 11.7% (± 4.1) in the upper half and approximately 2.1% (± 1.6) in the upper quarter. 42 days after partial bone marrow ablation, the whole bone volume was still increased by approximately 16.2% (± 0.5) and the lower half volume was increased by approximately 40.9% (± 3.4), the upper half volume by approximately 8.0% (± 2.2) and the upper quarter volume was completely normalized after 42 days (Figure 2.4b). Following intra-osseous injection of cancer cells, a tumor usually develops in the upper half of the bone.

Quantification of osteolysis induced volume changes

The relevance of volume measurements as a measure of cancer-induced osteolysis was tested. In addition, improvement of data quality was observed when a smaller pre-defined VOI around the area where osteolysis occurred was selected. This minimized
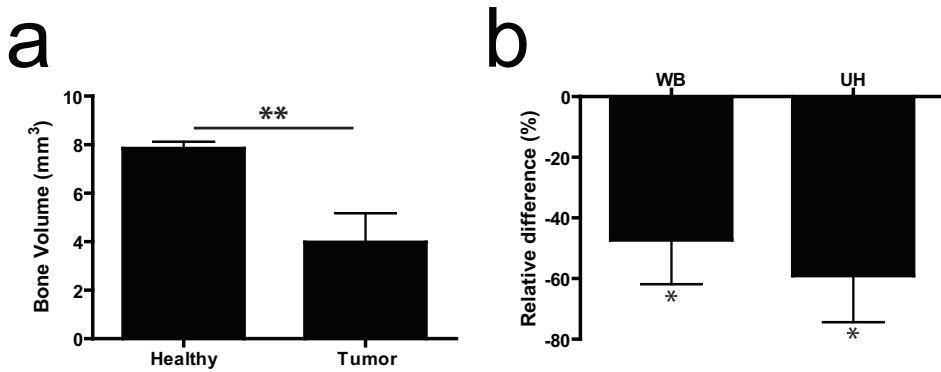
Figure 2.5: Quantification bone volume with and without osteolysis. (a) Bone volumes of the upper half of the tibia of healthy control limbs (left hind limbs) and tumor bearing limbs (right hind limbs) of the same animals, 42 days after tumor cell inoculations Error bars indicate SEM, $**: p < 0.01$. (b) Relative changes in bone volume between bones of healthy control limbs (left hind limbs) and tumor bearing limbs (right hind limbs) of the same animals, 42 days after tumor cell inoculations. The whole bone (WB) and upper half (UH) were measured in the same scans for comparison. By measuring a smaller VOI, the relative difference bone volume between the groups is enlarged. Both the WB and UH measurements were significantly different from 0, but the p-value was smaller for the UH measurement (p-values of 0.031 and 0.018 for the WB and UH measurement respectively). Error bars indicate SEM, $*: p < 0.05$.

the influence of the inoculation induced changes on volume measurements as well. Mice received an intra-osseous inoculation of MDA-BO2 cells, an osteolytic breast cancer cell line. The mice were sacrificed after 42 days, this is comparable to other experiments performed using this specific MDA subclone. [12–14] μCT scans were made of both hind limbs, with and without a tumor.

The volumes of the upper half of the tibiae were used to quantify the loss of bone volume in the diseased limbs compared to the healthy limbs (Figure 2.5a). The choice for measuring the upper half of the tibiae was based on the differential effects of the intra-osseous inoculation method on bone volume as described in Figure 2.4b and the localization of tumor growth after the inoculation procedure. The bone volume of the upper half decreased significantly compared to the same volume in the healthy bone.

Volume measurements of the whole bone and the upper half were compared to evaluate whether the selection of a smaller VOI improved data quality. Whole bone and upper half volume measurements were performed on the same μCT data sets to show the effect of selecting a smaller VOI and its impact on the decrease in bone volume. The osteolysis-induced bone loss was calculated as a percentage decrease in bone volume of the pathologic bone compared to the healthy bone. The volume of the whole osteolytic bones decreased by approximately 47% compared to the healthy control bones. This volume decrease was approximately 59% when measured in the
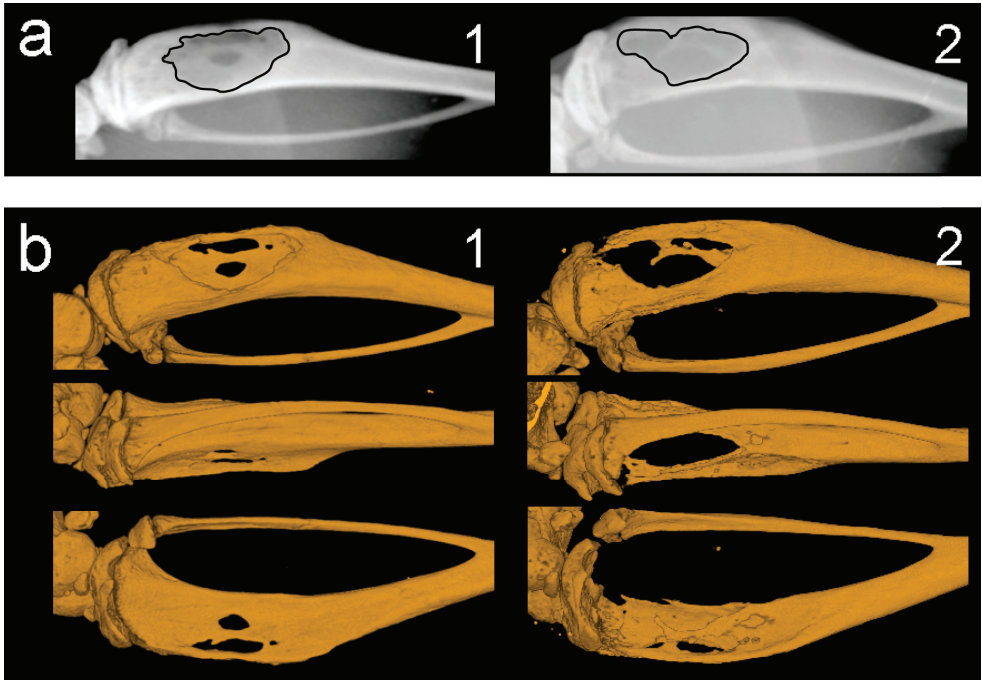
Figure 2.6: Radiography measurements are dependent on the projection. (a) Radiographs of two bones. The osteolytic lesion surface of bone #1 was 3420 pixels, the osteolytic lesion surface of bone #2 was 3402 pixels. (b) μCT scans of the same to bones as in (a). It can be concluded from the μCT scans by visual assessment that the osteolytic lesion in bone #1 is smaller than the osteolytic lesion in bone #2. Quantification of the upper half bone volume confirms this observation, the upper half volumes of bones #1 and #2 are 6.5mm^3 and 3.9mm^3, respectively. This example is illustrative for how the flattening of a 3D structure can result in incorrect observations.

upper half of the tibiae. In both cases the standard error of the mean was 15 (Figure 2.5b). These results indicate that volume differences can be magnified by selection of a smaller VOI, thereby improving the sensitivity of volume measurements as a method to quantify osteolysis.

Finally, radiographs of the osteolytic bones were made to show how the flattening of a 3D structure can influence measurements of osteolysis. To illustrate this problem, two bones with a comparable osteolytic surface on radiographs were selected for μCT analysis. The volumetric analysis of the μCT scans of these bones revealed that the osteolytic lesion of one bone was more severe than the other (Figure 2.6). The radiographs were acquired on one film simultaneously and processed identically.

Discussion

A new method to select VOIs and quantify bone volumes in a normalized way is presented in this study. Drugs and diseases can induce major structural changes in bone. Traditional quantification methods often use the growth plate as primary landmark which is often destroyed in cases of severe osteolysis. The current method reduces the dependency on this structure by using the knee and the branch point of tibia and fibula, two structures which are very unlikely to disappear. Moreover, performing the VOI selection relative to a centerline makes it possible to compensate for large structural deformations such as fractures and dislocations. Since all bone segments are presented in a normalized way, the user can indicate identical start and end planes to define a VOI in different scans. In addition, the use of a center-line enables the user to generate normalized sections that can be used to compare between scans or to compare scans with histological sections. The actual measurement of the selected volume is performed in the original scan to prevent measurement errors due to compression and/or expansion and errors in surface voxel definition that occur during reformation of a scan.

Osteolysis is currently quantified using radiography analysis. However, μCT scans are rarely used for quantification and instead they are used for visual representation as supportive data. One of the reasons for this is the lack of reliable methods for normalized processing of μCT scans. However, volume measurements can provide a valuable addition, not only for the quantification of osteolytic lesions, but for osteoblastic lesions as well. 2D radiographs are able to show the shadow projection of a bone with a specific 3D structure. The projection and flattening of a 3D structure can result in lesions projected on top of each other or along the side of the bone. However, the problem is that measurement errors are inadvertently introduced as shown in Figure 2.6. Moreover, volume measurements are not prone to observer bias when using detailed predefined definitions of a VOI relative to the bone.

Volume measurements can be used to quantify changes in bone volume of both osteolytic and osteoblastic lesions. This in contrast to 2D modalities which cannot be used to quantify subtle increases in bone volume. However, interpretation of the data becomes more complex in cases where both osteolytic and osteoblastic processes occur in the same bone. For instance, procedures commonly used to inoculate bones with cancer cells can induce changes in bone volume (Figure 2.4). As a result, measurements of the entire tibial volume can be misleading. We showed that the increase in bone volume mainly occurs in the lower half of the tibia. Thus, the effects of bone marrow ablation on the volume measurements can be minimized by limiting the VOI to the upper half of the tibia, which is the actual area of the bone where a tumor grows. This is an example of how careful selection of a VOI is crucial to generate reliable data.

Recent advances have been made in using μCT scans for the quantitative assessment of osteolysis. Johnson *et al.* followed bone loss over time in μCT scans made at multiple time points. The authors elegantly showed that there is no effect

of repeated X-ray exposure on tumor growth following their µCT scanning protocol. Using the entire bone volumes, they were able to visually detect osteolytic lesions one week after tumor cell inoculation and statistically differentiated lesions at week three more effectively than radiography.[15] It is feasible that the results from their study could be further improved by selection of a smaller VOI. As we have shown from our own study, the work of Johnson *et al.* could have also benefited from use of a smaller VOI. This could have eliminated the disruption of the volume measurements by other processes such as the direct effect of intra-osseous inoculations.

The relative change in bone volume is increased when measuring a smaller VOI, this while the standard error of the mean remains the same (Figure 2.5). Optimization of the measured VOI increases the sensitivity of volume measurements for detecting differences between osteolytic or osteoblastic lesion sizes. Observer bias is still minimal as the VOI is pre defined as a volume relative to the anatomy of the bone.

Other methods used to analyze smaller VOIs in µCT scans, which use a sub-volume instead of the entire bone volume, make use of a VOI with predefined dimensions. This VOI is 'a box' which is placed around a part of the scan. As a result, the selected VOI strongly depends on the scan orientation. Moreover, the curved shape of the tibia and possible fractures make it impossible to have two planes in a z-axis where both would cut the bone in a 90° angle. We eliminated these problems by using a VOI which is relative to the anatomy of the bone.

The reliable and reproducible selection of a VOI is pivotal when performing volume measurements in order to quantify the effects of osteolytic or osteoblastic effects. Here, we presented a curved planar reformation based approach to generate various normalized cross-sections. By using a reformatted space to select a VOI relative to the anatomy, we were able to eliminate measurement errors due to the orientation of the scan and deformations of the bone (e.g. dislocations, fractures). The effect of other processes elsewhere in the bone is eliminated by selecting a small VOI around the lesion. In conclusion, we found that by selecting a smaller VOI, the relative changes in bone volume are magnified which increases the sensitivity of our method of analysis as compared to other approaches.

Acknowledgments

References

1. Abrams HL, Spiro R, and Goldstein N. Metastases in carcinoma; analysis of 1000 autopsied cases. *Cancer*, 1950 Jan;3(1):74–85.

2. Clines GA and Guise TA. Hypercalcaemia of malignancy and basic research on mechanisms responsible for osteolytic and osteoblastic metastasis to bone. *Endocr Relat Cancer*, 2005 Sep;12(3):549–83.

3. Guise TA and Mundy GR. Cancer and bone. *Endocr Rev*, 1998 Feb;19(1):18–54.

4. Mundy GR. Metastasis to bone: causes, consequences and therapeutic opportunities. *Nat Rev Cancer*, 2002 Aug;2(8):584–93.

5. Nakai M, Mundy GR, Williams PJ, Boyce B, and Yoneda T. A synthetic antagonist to laminin inhibits the formation of osteolytic metastases by human melanoma cells in nude mice. *Cancer Res*, 1992 Oct;52(19):5395–9.

6. Sasaki A, Boyce BF, Story B, Wright KR, Chapman M, Boyce R, Mundy GR, and Yoneda T. Bisphosphonate risedronate reduces metastatic human breast cancer burden in bone in nude mice. *Cancer Res*, 1995 Aug;55(16):3551–7.

7. Peyruchaud O, Winding B, Pécheur I, Serre CM, Delmas P, and Clézardin P. Early detection of bone metastases in a murine model using fluorescent human breast cancer cells: application to the use of the bisphosphonate zoledronic acid in the treatment of osteolytic lesions. *J Bone Miner Res*, 2001 Nov;16(11):2027–34.

8. Wetterwald A, van der Pluijm G, Que I, Sijmons B, Buijs J, Karperien M, Löwik CWGM, Gautschi E, Thalmann GN, and Cecchini MG. Optical imaging of cancer metastasis to bone marrow: a mouse model of minimal residual disease. *Am J Pathol*, 2002 Mar;160(3):1143–53.

9. Arguello F, Baggs RB, and Frantz CN. A murine model of experimental metastasis to bone and bone marrow. *Cancer Res*, 1988 Dec;48(23):6876–81.

10. Patt HM and Maloney MA. Bone marrow regeneration after local injury: a review. *Exp Hematol*, 1975 Apr;3(2):135–48.

11. Bab I, Gazit D, Muhlrad A, and Shteyer A. Regenerating bone marrow produces a potent growth-promoting activity to osteogenic cells. *Endocrinology*, 1988 Jul;123(1):345–52.

12. Boucharaba A, Serre CM, Grès S, Saulnier-Blache JS, Bordet JC, Guglielmi J, Clézardin P, and Peyruchaud O. Platelet-derived lysophosphatidic acid supports the progression of osteolytic bone metastases in breast cancer. *J Clin Invest*, 2004 Dec;114(12):1714–25.

13. van der Pluijm G, Que I, Sijmons B, Buijs JT, Löwik CWGM, Wetterwald A, Thalmann GN, Papapoulos SE, and Cecchini MG. Interference with the microenvironmental support impairs the de novo formation of bone metastases in vivo. *Cancer Res*, 2005 Sep;65(17):7682–90.

14. Buijs JT, Que I, Löwik CWGM, Papapoulos SE, and van der Pluijm G. Inhibition of bone resorption and growth of breast cancer in the bone microenvironment. *Bone*, 2009 Feb;44(2):380–6.

15. Johnson LC, Johnson RW, Munoz SA, Mundy GR, Peterson TE, and Sterling JA. Longitudinal live animal micro-ct allows for quantitative analysis of tumor-induced bone destruction. *Bone*, 2011 Jan;48(1):141–51.